© 2018. Published by The Company of Biologists Ltd | Development (2018) 145, dev166975. doi:10.1242/dev.166975

STEM CELLS AND REGENERATION

RESEARCH ARTICLE

Simplet-dependent regulation of β-catenin signaling influences skeletal patterning downstream of Cx43

Shashwati Bhattacharya, Domenic Gargiulo and M. Kathryn Iovine*

ABSTRACT

The correct positioning of joints in the vertebrate skeleton is not well understood. Mutations in *connexin43* (*cx43*) cause the short segment phenotype of the zebrafish *short fin* (*sof*^{b123}) mutant. We have shown that Cx43 suppresses *evx1* expression, a transcription factor required for joint formation. Here, we provide novel insights into how Cx43 influences *evx1* transcription. First, we find that Simplet (Smp) knockdown recapitulates the *sof*^{b123} phenotypes of reduced regenerate length and reduced segment length, and we find evidence for synergy between *cx43* and *smp*. Moreover, knockdown of Smp increases the *evx1* expression, similar to *cx43* knockdown. Previous studies have shown that Smp is required for the nuclear localization of β-catenin. Indeed, β-catenin activity is required for segment length, and is reduced in both *sof*^{b123} mutants and following Smp knockdown in regenerating fins. We further show that blocking canonical Wnt signaling results in a synergistic reduction in segment length in *sof*$^{b123/+}$ heterozygotes. Together, our findings suggest that both Smp and β-catenin function in a common molecular pathway with *cx43* to influence both *evx1* expression and joint location.

KEY WORDS: Joint morphogenesis, Cx43, Evx1, Fin regeneration, Simplet, β-Catenin

INTRODUCTION

The correct placement of joints is required for skeletal flexibility and functionality. However, the mechanisms by which joints are correctly positioned in the skeleton are poorly understood. We use the zebrafish regenerating caudal fin as the model system in which to address this fundamental issue. The caudal fin is composed of 16-18 fin rays, and each fin ray is composed of bony segments flanked by joints. The main advantages of this system include that the fin is a rich source of joints, that the amputated fin regenerates rapidly and that the early stages of joint morphogenesis in the fin ray resemble the early stages of mammalian joint formation (Sims et al., 2009).

The fin rays are made of two hemirays of bone matrix surrounding a central mesenchyme of undifferentiated fibroblasts. The dividing cells are located in the distal mesenchyme, whereas the differentiating osteoblasts are located in the lateral mesenchyme. Actinotrichia are produced at the distal ends of each fin ray. Actinotrichia are collagen-like fibrils where the osteoblasts align and secrete the bone matrix, or lepidotrichia (Becerra et al., 1983). Osteoblasts and joint-forming cells are derived from common precursor cells (Tu and Johnson, 2011), located distally and laterally. We refer to this population of cells collectively as the 'skeletal precursor cells'. The fin regenerates in the proximal-to-distal direction, with new segments continually added to the distal end of the fin ray. Therefore, the newer joints are always located distal to the older joints. This system permits the study of joint morphogenesis over time (Sims et al., 2009; Dardis et al., 2017). Joint initiation occurs when a single row of joint-forming cells aligns at the site of the presumptive joint. As the joint matures, joint-forming cells appear to move apart, forming two rows of cuboidal cells. These cells resemble the interzone cells of mammalian synovial joints because of their appearance at the site of the future joint and by their apparent ability to contribute to joint morphogenesis (Pacifici et al., 2006). Thus, the appearance of the interzone indicates that a joint will be produced at a specified location, and the cells of the interzone help to build the physical joint. It is unclear when the molecular pathways for determining joint location are mechanistically separable from the molecular pathways for building the joint. We refer to pathways that influence joint initiation as regulating joint location. Alternatively, if the affected pathway is unclear we instead use the more general term 'joint formation'.

Previous studies in the zebrafish fin length mutants *short fin* and *another long fin* (*sof*^{b123} and *alf*^{dty86}) revealed that the gap junction protein connexin 43 (Cx43) plays important roles in determining the location of joints. Hypomorphic mutations in *cx43* cause the *sof*^{b123} phenotypes of shorter fin length, reduced cell proliferation and shorter segment length (Iovine et al., 2005). Cx43-knockdown (KD) also recapitulates the *sof*^{b123} phenotype (Hoptak-Solga et al., 2008). The *alf*^{dty86}mutant, in contrast, exhibits stochastic joint failure and longer segments, on average (Sims et al., 2009). Interestingly, although the mutation causing the *alf*^{dty86} phenotypes is not in the *cx43* gene (Perathoner et al., 2014), *alf*^{dty86} mutants exhibit increased *cx43* mRNA expression. Moreover, Cx43 KD in *alf* rescues the irregular segment length phenotype (Sims et al., 2009). Together, these studies provide evidence that Cx43 inhibits joint formation in zebrafish fin. Indeed, more recent studies have identified a transient reduction in *cx43* expression coincident with joint initiation (Dardis et al., 2017). From these and other studies, we suggest that the short segment phenotype of *sof*^{b123} is due to premature joint initiation, whereas the long segment phenotype of *alf*^{dty86} is due to a failure of joint initiation. Thus, for Cx43-dependent phenotypes, segment length is a proxy for joint location.

The transcription factor *evx1* is required for joint formation (Schulte et al., 2011) and low levels of *evx1* expression precede joint initiation (Dardis et al., 2017). Interestingly, expression of *evx1* is premature in *sof*^{b123} and sporadic in *alf*^{dty86} (Ton and Iovine, 2013b), consistent with our model for segment length phenotypes in these mutants. Moreover, Cx43 KD rescues *evx1* expression in *alf*^{dty86} mutants (Ton and Iovine, 2013b). Therefore, we suggest that Cx43 influences segment length by influencing the timing of *evx1* expression, which in turn influences the location of the next joint. Cx43 is expressed

Department of Biological Sciences, Lehigh University, Bethlehem, PA 18015, USA.

*Author for correspondence (mki3@lehigh.edu)

M.K.I., 0000-0003-0046-8482

Received 23 April 2018; Accepted 24 October 2018

Development (2018) 145, dev166975. doi:10.1242/dev.166975

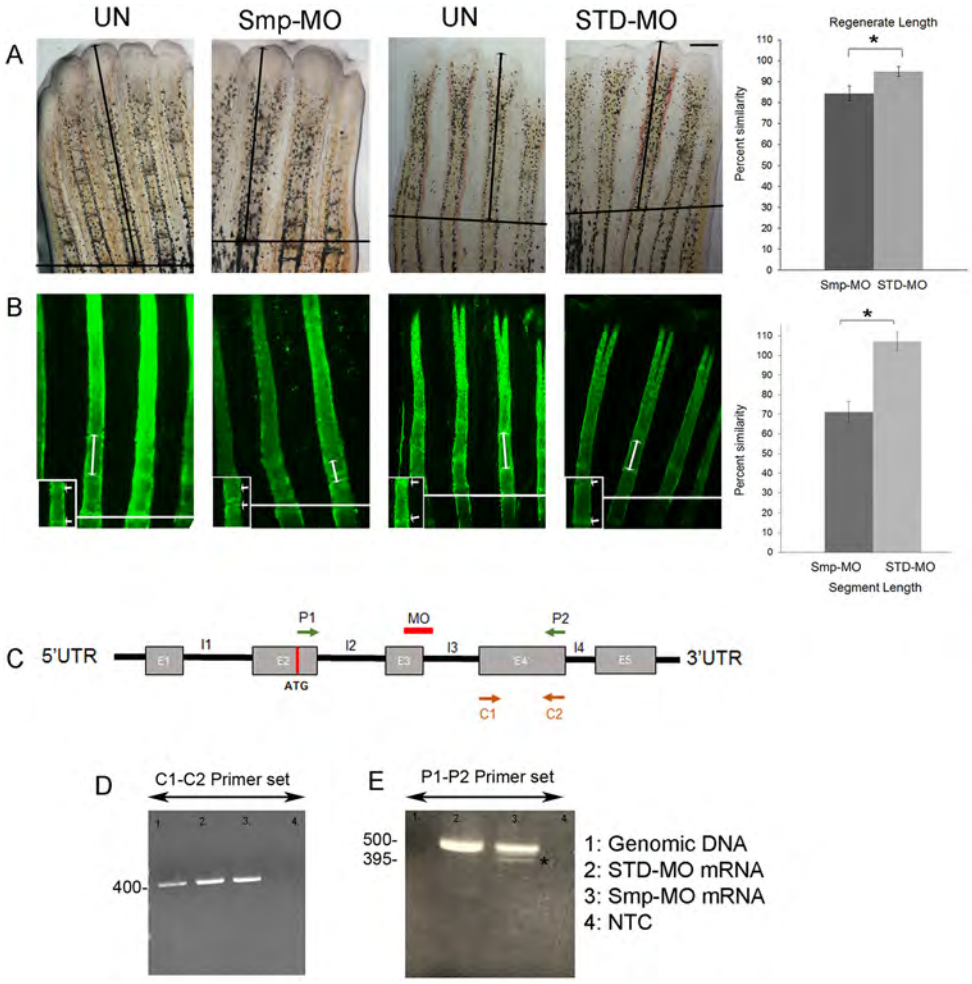

Fig. 1. The Smp-KD phenotypes include significantly reduced segment length and regenerate length. (A) Regenerate length is reduced in Smp-MO-treated fins compared with STD-MO-treated fins. All fins were amputated at the 50% level. The amputation plane is indicated (black line). The black arrow indicates the distance from the amputation plane to the distal tip of the 3rd fin ray. Graph shows significant reduction in percentage similarity in Smp-MO- and STD-MO-injected fins (*P<0.05, Student's t-test, two-tailed and unpaired). Three independent trials were performed (n=25 total per treatment). The data did not differ significantly from normality (Shapiro-Wilk's test, P>0.05). Error bars represent s.e.m. (B) Calcein-stained fin rays show reduced segment length in Smp-MO-treated fins compared with STD-MO-treated fins. Double-headed arrows indicate the first completed segment following the amputation plane (white line). The inset shows a higher magnification of the segments (arrows indicate joints). Graph reveals significant reduction in percentage similarity in Smp-MO- and STD-MO-injected fins (*P<0.05, Student's t-test, two-tailed and unpaired). Three independent trials were performed (n=25 total per treatment). The data did not differ significantly from normality (Shapiro-Wilk's test, P>0.05). Error bars represent s.e.m. (C) Schematic representation of zebrafish *smp* pre-mRNA. The exons are shown in gray boxes and the introns are drawn as black lines. Positions of the MO and of the primers are indicated. The MO is predicted to cause skipping of exon 3 (55 bp). (D) Results of the RT-PCR analysis using C1-C2 primer set (396 bp product is predicted). (E) Results of the RT-PCR analysis using P1-P2 primer set reveals reduced full-length product and Smp-MO-dependent presence of the shorter product. The P1-P2 primer pair amplified product (380 bp) in lane 3 marked with an asterisk is caused by the skipping of exon 3 compared with lane 2, where exon 3 was included (435 bp). Scale bar: 50 µm.

both in the medial mesenchyme and in the distal-most joint-forming cells (Sims et al., 2009). However, we have found that Cx43 function in the medial mesenchyme, and not in the lateral cells, is capable of rescuing the short segment phenotype of sof^{b123} mutants (Dardis et al., 2017). Therefore, our current model is that Cx43 function in the medial mesenchyme influences cell fate decisions in the lateral skeletal precursor cells. High *cx43* expression favors differentiation of bone-forming cells (i.e. low *evx1* and joint pathway off), whereas transient reductions in *cx43* expression favors differentiation of joint-forming cells (i.e. increased *evx1* and joint pathway on) (Dardis et al., 2017).

The findings in this article contribute to our understanding of how Cx43 influences *evx1* expression and cell fate decisions in the lateral skeletal precursor cells. We find that Simplet (Smp) and β-catenin signaling mediates Cx43-dependent expression of *evx1*. Smp, or Fam53b, is a protein of 407 amino acids containing a 14-3-3 binding motif and a nuclear localization signal (NLS). Prior studies suggest that Smp regulates cell proliferation during early developmental stages of Medaka development (Thermes et al., 2006) and in regenerating fins (Kizil et al., 2009). More recently, Smp has been shown to influence the nuclear localization of β-catenin in zebrafish embryos (Kizil et al., 2014). Here, we show that *smp* is expressed downstream of Cx43, and that Smp is required for segment length and *evx1* expression. We similarly find that β-catenin is required for segment length and *evx1* expression, and that β-catenin signaling is reduced in both sof^{b123} and in Smp KD regenerating fins. These findings provide compelling evidence that Smp and β-catenin

Development (2018) 145, dev166975. doi:10.1242/dev.166975

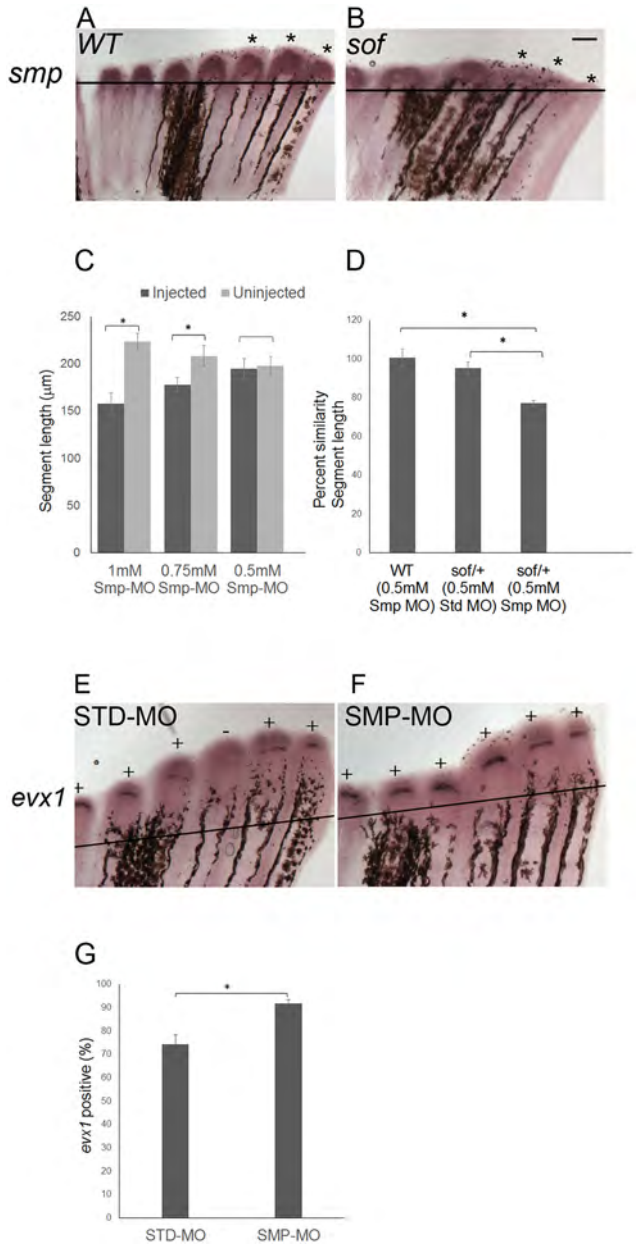

Fig. 2. *smp* and *cx43* function in a common pathway to influence *evx1* expression. (A) Wild-type and (B) *sof*^{b123} fins were amputated at 50% and permitted to regenerate for 87 h. At 87 hpa, the fins were harvested and processed for *smp* whole-mount *in situ* hybridization. Asterisks represent the expression domains of *smp* in each of the three fin rays. Three independent trials were performed (n=18 per genotype). (C) Smp-MO concentrations of 1 mM (n=6), 0.75 mM (n=6) and 0.5 mM (n=11) were used to identify the subthreshold concentration. The 0.5 mM concentration of Smp-MO was selected as the subthreshold dose, as there is no significant decrease in the segment length. The data did not differ significantly from normality (Shapiro-Wilk's test, P>0.05). Error bars represent s.e.m. Student's t-test was performed to test for significance (two-tailed and unpaired, *P<0.05). (D) Synergistic effects of the 0.5 mM dose of Smp-MO with *sof*^{b123} heterozygotes (n=10) are revealed compared with either wild-type fins (n=11) injected with 0.5 mM Smp-MO or with *sof*$^{b123/+}$ heterozygotes injected with STD-MO (n=7). The data do not differ significantly from normality (Shapiro-Wilk's test, P>0.05). Error bars represent s.e.m. Student's t-test was performed to test for significance (two-tailed and unpaired, *P<0.05). (E,F) Whole-mount *in situ* hybridization shows that the frequency of *evx1* expression is increased in Smp-MO fins (n=21 fins) compared with the STD-MO fins (n=22 fins) (three biological replicates). All fin rays across the fins were injected with Smp-MO or STD-MO at 72 hpa and harvested at 87 hpa. Plus indicates fin rays positive for *evx1*; minus indicates fin rays negative for *evx1*. (G) The Smp-MO fins show an increased frequency of *evx1*-positive fin rays compared with STD-MO injected fins. The data did not differ significantly from normality (Shapiro-Wilk's test, P>0.05). Error bars represent s.e.m. Student's t-test was performed to test for significance (two-tailed and unpaired, *P<0.05). Scale bar: 50 μm.

function downstream of Cx43 to influence joint location through the regulation of *evx1* expression.

RESULTS

smp and *cx43* function in a common pathway to regulate joint location

Smp has been shown to regulate cell proliferation during zebrafish caudal fin regeneration (Kizil et al., 2009). Expression of *smp* is observed in the distal epidermis, and also in both the distal and lateral mesenchyme (Kizil et al., 2009), and could contribute to joint formation. To test this possibility, we completed morpholino (MO)-mediated gene knockdown (KD) of Smp using one of the two morpholinos previously validated for Smp KD (i.e. Smp-1, Exon3–Intron3 splice antisense MO; Kizil et al., 2009). We first demonstrated that this MO appropriately targets *smp* mRNA by interfering with correct splicing (Fig. 1). This MO is predicted to cause skipping of exon 3, which we observed in Smp-MO-treated fins but not in standard control MO (STD-MO)-treated fins.

We next tested for skeletal phenotypes during regeneration. We injected the Smp-MO into half of the fin rays of wild-type regenerating fin at 72 h post-amputation (hpa), leaving the other half as an internal control. Alternatively, STD-MO was similarly injected. After injection, the whole fin was electroporated to induce cellular uptake of the fluorescein-labeled MO. Successful injection/electroporation was determined by observing fluorescein signal at 24 h post-electroporation (hpe) (Thummel and Iovine, 2017). Regenerate length and segment length were evaluated at 4 dpe (i.e. 7 dpa), and measurements were taken from the 3rd fin ray, which we use as a standard (Iovine and Johnson, 2000). We use the percentage similarity method to determine whether the gene-targeting MO has an effect (i.e. Banerji et al., 2017; Govindan et al., 2016). With this method, we take the ratio of the injected side over the uninjected side and multiply by 100, and we compare these values for the Smp-MO- and for the STD-MO-treated fins (values close to 100% indicate little effect of the MO; values with low similarity indicate that the MO had an effect). This method reduces the effect of fin to fin variation. Importantly, we observed significant reduction in regenerate length in Smp-KD compared with the STD-MO (Fig. 1), recapitulating the published phenotype for Smp-KD (Kizil et al., 2009). We further showed that Smp-KD leads to reduced segment length (Fig. 1), similar to *sof*^{b123} mutants and to Cx43-KD.

To test whether *smp* is expressed downstream of *cx43*, we performed whole-mount *in situ* hybridization in 5 dpa wild-type and *sof*^{b123} regenerating fins. We found that *smp* expression is reduced in *sof*^{b123} compared with wild type (Fig. 2). This finding was confirmed through qRT-PCR (Table 1 and Fig. S1). Together, these findings suggest that *smp* acts downstream of *cx43* to influence segment length.

Based only on the observed differences in gene expression, it is difficult to distinguish between *smp* expression being reduced within all cells in *sof*^{b123} regenerating fins, or *sof*^{b123} exhibiting fewer *smp*-positive cells. To test whether *smp* and *cx43* work in the same pathway to regulate joint formation, we tested for synergy of the two gene products. First, we identified the subthreshold concentration of the Smp-MO by injecting/electroporating morpholino concentrations of 1 mM (typical dose), 0.75 mM and

Development (2018) 145, dev166975. doi:10.1242/dev.166975

Table 1. Quantitative RT-PCR results

Gene	Condition	Average C_T	Average *keratin* C_T	ΔC_T gene of interest-*keratin*	ΔC_T standard MO/wild type-*keratin*	$\Delta\Delta C_T$ $\Delta C_{T\ (expt)}$-$\Delta C_{T\ (control)}$	Fold difference
axin2	*sof*	23.40±0.145	15.828±0.084	7.573±0.168	6.77±0.1433	0.8±0.22	0.574 (0.49-0.66) relative to wild type
axin2	Smp-KD	20.38±0.178	13.29±0.136	7.08±0.22	6.26±0.36	0.82±0.42	0.605 (0.42-0.76) relative to STD-MO
smp	*sof*	23.77±0.23	16.93±0.08	6.84±0.25	6.22±0.322	0.61±0.40	0.65 (0.49-0.86) relative to wild type
evx1	Smp-KD	24.13±0.38	13.75±0.20	10.38±0.43	11.82±0.15	−1.44±0.45	2.71 (1.97-3.73) relative to STD-MO
evx1	IWR1	28.49±0.17	19.95±0.184	8.533±0.256	8.8±0.517	−0.267±0.57	1.203 (0.8-1.79) relative to DMSO

The ΔC_T value is determined by subtracting the average keratin C_T value from the average gene C_T value. The standard deviation of the difference is calculated from the standard deviations of the gene and keratin values using the comparative method.
The calculation of the $\Delta\Delta C_T$ involves subtraction of the ΔC_T calibrator value. This is a subtraction of an arbitrary constant, so the deviation of $\Delta\Delta C_T$ is the same as the standard deviation of the ΔC_T value.
The range given for a gene relative to standard-MO is determined by evaluating the expression $2^{-\Delta\Delta CT}$ with $\Delta\Delta C_T$ +s and $\Delta\Delta C_T$ −s, where s=the standard deviation of the $\Delta\Delta C_T$ value.
At least three biological replicates were performed for all comparisons. The fold-change values did not differ significantly from normal and were statistically significant when compared with their respective control (Student's *t*-test, $P<0.05$).

0.5 mM in 3 dpa regenerating fins, and measuring segment length at 7 dpa. We identified the 0.5 mM concentration of Smp-MO as the subthreshold dose (Fig. 2). We next completed KD using this dose of MO in $sof^{b123/+}$ heterozygous fins, as sof^{b123} is recessive and therefore represents a subthreshold activity of *cx43*. If *smp* and *cx43* function in a common pathway, we expected to find a significant decrease in segment length in $sof^{b123/+}$ fins injected with 0.5 mM Smp-MO. Indeed, we found that there is a significant decrease in the segment length in $sof^{b123/+}$ fins injected with 0.5 mM Smp-MO compared with either the STD-MO injected in $sof^{b123/+}$ fins or with 0.5 mM Smp-MO injected into wild-type fins (Fig. 2). These findings provide evidence for synergy, supporting the conclusion that *smp* and *cx43* function together in a common molecular pathway to regulate joint formation.

Previous studies have shown that Cx43 suppresses *evx1* (Dardis et al., 2017). Expression of *evx1* is observed in a discrete row of joint-forming cells at the distal ends of the regenerating fin in many, but not typically all, fin rays (Ton and Iovine, 2013b). Therefore, one way to evaluate changes in *evx1* expression is to calculate the frequency of *evx1*-positive fin rays across regenerating fins (Ton and Iovine, 2013b; Dardis et al., 2017). An increase in the percentage of *evx1*-positive fin rays reflects abrogation of *evx1* suppression. To investigate whether *smp* similarly inhibits *evx1* expression, we monitored the percentage of *evx1*-positive fin rays in fins treated with Smp-MO compared with STD-MO. The percentage of *evx1*-positive fin rays increased in the Smp-KD fins compared with the STD-MO fins (Fig. 2), strongly suggesting that *smp* suppresses *evx1*. We validated this result through qRT-PCR, which also showed increased *evx1* expression in Smp-KD fins compared with the fins treated with STD-MO (Table 1 and Fig. S1). Together, the reduced expression of *smp* in sof^{b123} regenerating fins, the evidence for synergy between *cx43* and *smp*, and the fact that both *cx43* and *smp* negatively regulate *evx1* expression in skeletal precursor cells, strongly suggests that *cx43* and *smp* act in a common pathway to influence joint location.

Active levels of β-catenin are reduced in both sof^{b123} and Smp-KD regenerating fins

It was previously shown that Smp influences β-catenin nuclear localization during zebrafish development (Kizil et al., 2014), and that β-catenin signaling contributes to regenerate length (Wehner et al., 2014). Furthermore, β-catenin activity and protein localize to the distal-most blastema as well as to the lateral skeletal precursor cells (Wehner et al., 2014; Stewart et al., 2014). Therefore, we tested whether β-catenin signaling is involved in joint formation using two independent inhibitors of canonical Wnt signaling. IWR-1 interacts with and stabilizes axin directly (Chen et al., 2009). XAV939 binds and inhibits Tankyrase enzymes that inhibit axin, and therefore similarly leads to axin stabilization (Huang et al., 2009). Both IWR-1 and XAV939 enhance β-catenin degradation (Huang et al., 2009; Chen et al., 2009). To test whether these inhibitors influence joint formation, we amputated wild-type fins at 50%. At 72 h post-amputation (hpa), fish were treated with either 10 µM IWR-1 (versus DMSO alone) or with 5 µM XAV939 (versus DMSO alone) for 3 days (changing the water and treatment each day). We observed a significant reduction in both regenerate length and in segment length using each drug (Fig. 3). The *axin2* gene is a direct target of canonical Wnt signaling, and is often used as a readout of β-catenin signaling (Jho et al., 2002). Therefore, effects on β-catenin signaling following drug treatment were confirmed by demonstrating reduced expression of the target gene *axin2* (Fig. 4). These findings suggest that, in addition to influencing cell proliferation, β-catenin also inhibits joint formation.

Next we tested whether β-catenin activity is reduced in sof^{b123} and in Smp-KD regenerating fins. The active form of β-catenin is the non-phosphorylated form, which can be detected with a specific antibody (Moorer et al., 2017). We first examined the amount of active β-catenin using immunoblotting. We found that the amount of active β-catenin is decreased in sof^{b123} lysates by about 52%±18 compared with wild-type lysates, and, similarly, in Smp-KD fins lysates by about 37%±8 compared with STD-MO-treated fins (Fig. 4).

To confirm that active β-catenin signaling is reduced in sof^{b123}, we monitored *axin2* expression. Importantly, *axin2* expression is decreased in sof^{b123} compared with wild type by both *in situ* hybridization (Fig. 4) and qRT-PCR (Table 1 and Fig. S1). We similarly found reduced *axin2* expression in Smp-KD fins compared with the STD-MO-treated fins (Table 1 and Fig. S1). These findings support the conclusion that β-catenin signaling occurs downstream of both Cx43 and Smp.

β-Catenin and Cx43 regulate joint location through a common molecular pathway

Next we tested whether β-catenin and Cx43 function in the same pathway by testing for synergy between sof^{b123}/+ and IWR-1. We first identified 8 µM IWR-1 as the subthreshold dose (Fig. 5). We next tested this concentration in $sof^{b123/+}$ heterozygous fish. We observed a significantly reduced segment length in $sof^{b123/+}$ treated with 8 µM IWR1 compared with either the 8 µM IWR-1 dose in wild type (i.e. the subthreshold dose) or with DMSO alone in $sof^{b123/+}$ (i.e. demonstrating DMSO alone had no effect) (Fig. 5).

Development (2018) 145, dev166975. doi:10.1242/dev.166975

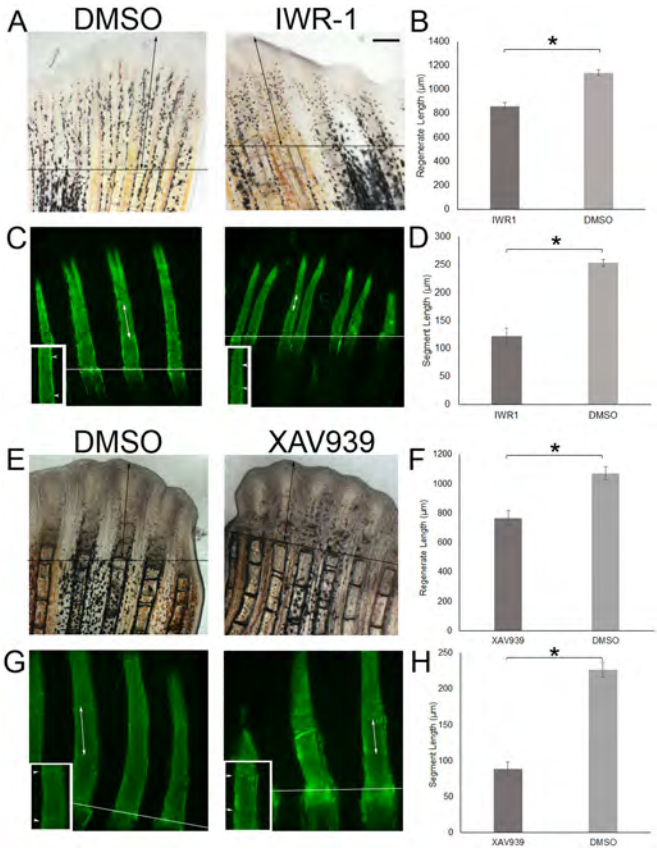

Fig. 3. β-Catenin regulates regenerate length and segment length. (A,B,E,F) Wild-type fish at 72 hpa were treated with IWR-1 (10 µM) compared with DMSO for 3 days (*n*=13 per treatment) or with XAV939 (5 µM) compared with DMSO for 3 days (*n*=16 per treatment). The same fins were used to measure regenerate length and segment length. Regenerate length was reduced in drug-treated fins compared with DMSO-treated fins. (C,D,G,H) Segment length was reduced in drug-treated fins compared with DMSO-treated fins. The amputation plane is identified by the horizontal line, and the double-headed arrows identify regenerate length in the top panels and segment length in the bottom panels. Insets in C and G show the measured segment at a higher magnification (arrowheads indicate joints). There is a significant reduction in regenerate length (B,F) and segment length (D,H). The data in B,D,F,H do not differ significantly from normality (Shapiro-Wilk's test, $P>0.05$). Error bars represent s.e.m. Student's *t*-test was performed to test for significance (two-tailed and unpaired, $*P<0.05$). Scale bar: 50 µm.

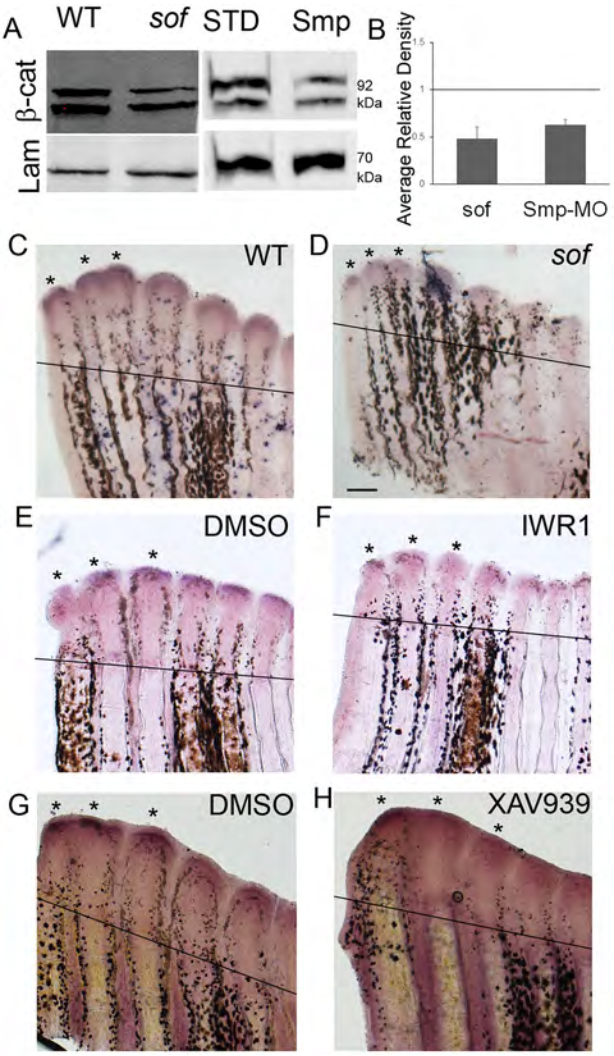

Fig. 4. Active β-catenin requires Smp and Cx43. (A) Immunoblots of wild-type fin lysates compared with *sof*^{b123} fin lysates, and STD-MO fin lysates compared with Smp-MO fin lysates. Immunoblots were probed with active (non-phosphorylated) anti β-catenin antibody and with Lamin a/c antibody. (B) Graph showing the average relative densities of the β-catenin bands between experimental and control samples from three biological replicates. The amount of active β-catenin is reduced by 52% in *sof*^{b123} lysates, and by 37% in Smp-MO lysates. Error bar represents s.e.m. (C-H) *axin2* expression by *in situ* hybridization in wild-type versus *sof* 5 dpa regenerating fins (C,D, *n*=10 for each); DMSO versus IWR-1-treated 5 dpa regenerating fins (E,F, *n*=10 for each); DMSO versus XAV939-treated 5 dpa regenerating fins (G,H, *n*=10 for each). Asterisks represent the expression domains of *axin2* in each of three fin rays. The black line represents the amputation plane. Scale bar: 50 µm.

These data provide evidence that canonical Wnt signaling acts in a common pathway with Cx43 to influence joint formation.

Finally, we further tested whether β-catenin signaling influences *evx1* expression. We measured levels of *evx1* via qRT-PCR in IWR-1-treated fins compared with DMSO-treated fins. We found that IWR-1-treated fins indeed have higher levels of *evx1* expression compared with DMSO-treated fins (Table 1 and Fig. S1). Together with our previous findings, these results suggest that Cx43, Smp and β-catenin act in a common pathway to inhibit *evx1* expression and thereby regulate joint location.

DISCUSSION

We are interested in providing insights into the molecular mechanism of joint formation and, more specifically, on how joint location is selected. In our previous studies, we explored cellular changes that occur during joint morphogenesis (Sims et al., 2009), we identified a molecular pathway occurring downstream of Cx43 that influences joint formation (Ton and Iovine, 2012; Ton and Iovine, 2013b), we found that Cx43 function in the medial fibroblasts is responsible for joint formation (Dardis et al., 2017) and we showed that Cx43 suppresses both *evx1* expression and joint initiation (Ton and Iovine, 2013b; Dardis et al., 2017). Here, we provide new insights into how Cx43 suppresses *evx1* expression. First, we showed that *smp* is downstream of *cx43* and functions synergistically with *cx43* to suppress *evx1* in the joint formation pathway. Smp has been shown to influence the nuclear localization of β-catenin in zebrafish embryos (Kizil et al., 2014). Therefore, we tested whether β-catenin influences segment length, and showed that β-catenin functions in a common pathway with Cx43 to influence joint location and *evx1* expression. Furthermore, we

Development (2018) 145, dev166975. doi:10.1242/dev.166975

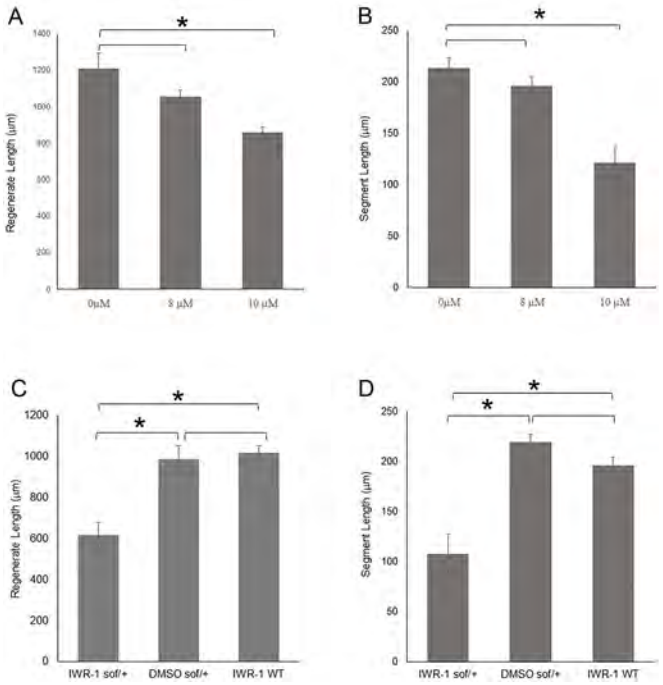

Fig. 5. β-Catenin and Cx43 function in a common molecular pathway. (A,B) Different concentrations of IWR-1 were used to identify the subthreshold dose on both regenerate length and segment length (8 µM concentration was selected for both) (n=13 fins per treatment). (C,D) Synergistic effects were identified for 8 µM IWR-1 in *sof*$^{b123/+}$ heterozygotes (n=14) compared with either 8 µM IWR-1 in wild-type (n=17) or to DMSO alone in *sof*$^{b123/+}$ heterozygotes (n=13) on both regenerate length and segment length. The data did not differ significantly from normality (Shapiro-Wilk's test, P>0.05). Error bars represent the s.e.m. Student's t-test was performed to test for significance (two-tailed and unpaired, *P<0.05).

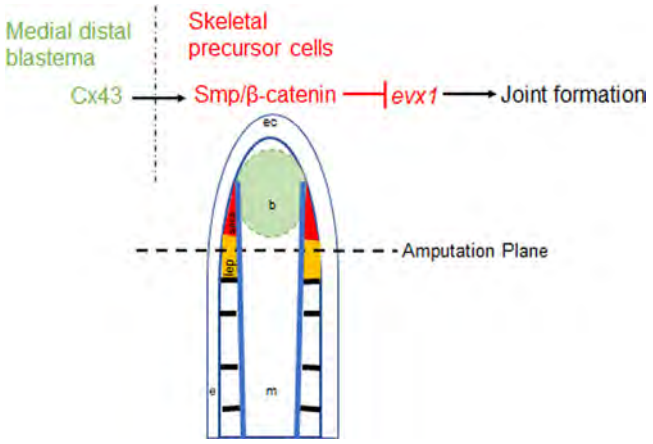

Fig. 6. Model for the role of Cx43 during joint formation. Cx43 expression in the medial mesenchyme influences joint formation in the lateral skeletal precursor cells (see Dardis et al., 2017). Here, we show that Cx43 influences *smp* expression, which in turn influences β-catenin signaling in the skeletal precursor cells. We propose that Smp/β-catenin suppress *evx1*. Thus, high levels of Cx43 favor bone formation (and inhibit *evx1*), whereas reduced levels of Cx43 permit *evx1* expression by relieving Smp/β-catenin inhibition.

showed that active-β-catenin, which translocates to the nucleus to transcribe Wnt target genes, is reduced in both *sof*^{b123} and Smp-MO lysates. Reduced *axin2* expression in *sof*^{b123} and Smp-MO-treated fins confirmed that β-catenin signaling is reduced when either Cx43 or Smp function is reduced. From these findings, we propose a model that Cx43 activity influences β-catenin activity through regulation of *smp* expression in the skeletal precursor cells (Fig. 6). The *smp* gene is expressed more broadly than the skeletal precursor cells (Kizil et al., 2009). However, the β-catenin activity that contributes to the fin skeleton is found mainly in the lateral mesenchyme (Stewart et al., 2014; Wehner et al., 2014), and *evx1* expression is restricted to a subset of the skeletal precursor cells (Ton and Iovine, 2013b). Thus, the most parsimonious explanation of our results is that the Cx43-dependent upregulation of *smp* facilitates an increase in nuclear β-catenin (i.e. via the Smp-NLS; Kizil et al., 2014), and suppression of *evx1* expression in skeletal precursor cells. The transient decrease in *cx43* expression coincident with joint initiation (described by Dardis et al., 2017) thereby relieves the Cx43/Smp/β-catenin inhibition on *evx1* and permits joint formation.

Findings by others have shown that Wnt/β-catenin signaling is responsible for regulating blastemal cell proliferation (Wehner et al., 2014; Stoick-Cooper et al., 2007), for patterning the epidermis (Wehner et al., 2014), for maintaining the population of pre-osteoblasts (Stewart et al., 2014) and for promoting osteoblast differentiation via BMPs (Stewart et al., 2014). Our findings provide additional support for the role of Wnt/β-catenin during cell proliferation and in promoting osteoblast differentiation, and we further demonstrate that Wnt/β-catenin influences joint location. Thus, we extend previous studies by demonstrating that Wnt/β-catenin influences a cell-fate decision (i.e. between the osteoblast fate versus the joint-forming cell fate) in the skeletal precursor cells, favoring the osteoblast cell fate by inhibiting *evx1* expression. We further provide evidence that this function of β-catenin occurs downstream of Cx43 and Smp. BMP signaling was also reported to occur downstream of Wnt/β-catenin, promoting continued differentiation of the osteoblast lineage (Stewart et al., 2014). It will be of interest to determine whether BMP signaling similarly inhibits the differentiation of joint-forming cells.

This model of Cx43 and β-catenin cooperating to inhibit joint formation is also supported in other model systems. In primary rat BMSCs, Cx43 increases with osteoblast differentiation, and KD suppresses both differentiation and β-catenin expression/activation (Lin et al., 2018). Further, Cx43 has been shown to promote β-catenin signaling in developing rabbit (Liu et al., 2016) and mouse (Moorer et al., 2017) skeletons, although the mechanism(s) of this regulation may not be transcriptional. For example, in the latter study the Cx43 C terminus was shown to serve as a docking platform for signaling molecules, and appears to be required for the full activity of such signaling pathways, including β-catenin (Moorer et al., 2017). Direct interactions between the Cx43 C terminus and β-catenin have been revealed (Spagnol et al., 2018). Moreover, Wnt/β-catenin signaling is absent in the cells of the mammalian joint interzone, and reducing β-catenin in these early skeletal elements activity similarly expands joint cell markers (Yamagami et al., 2009). These findings are consistent with β-catenin serving as a conserved negative signal for joint formation. Interestingly, others have also found that β-catenin signaling may promote *cx43* transcription (Xia et al., 2010; Mureli et al., 2013), suggesting the possibility of positive feedback.

Several questions remain unanswered. For example, as Cx43 function in the medial fibroblasts is responsible for regulating the joint cell fate in the lateral skeletal precursor cells (Dardis et al., 2017), how is *smp* expression regulated by Cx43? Possible answers include that heterotypic gap junction channels are formed between Cx43 and another unidentified connexin in the skeletal precursor cells, and/or that Cx43-positive cells release a secreted growth factor

Development (2018) 145, dev166975. doi:10.1242/dev.166975

that stimulates changes in gene expression in the skeletal precursor cells (also discussed by Ton and Iovine, 2013a). The mechanism for how Smp/β-catenin suppresses *evx1* also requires elucidation. β-Catenin (alone, or possibly with Smp) may function as a direct repressor of *evx1*. β-Catenin has been shown to bind to the *Evx1* promoter during gastrulation in the mouse (Funa et al., 2015), and this interaction may be conserved. Alternatively, β-catenin (i.e. ±Smp) may instead increase the expression of a repressor that, in turn, negatively regulates *evx1*. Importantly, a recent study identified a candidate transcription factor, *hoxa13a*, that may act upstream of *evx1* during the specification of joint-forming cells (McMillan et al., 2018). It will be of interest to discover the direct targets of nuclear β-catenin during this process. Future studies will address these and other issues regarding the mechanism of Cx43-dependent inhibition of joint formation.

MATERIALS AND METHODS

Fish maintenance

Zebrafish (*Danio rerio*) were maintained in circulating water system built by Aquatic Habitats (now Pentair). Zebrafish were kept at 27-28°C in a 14:10 h light:dark period (Westerfield, 1993). The quality of the fish tank water was monitored and dosed to maintain conductivity (400-600 mS) and pH (6.95-7.30). Research was performed according to the IACUC for Lehigh University (protocol #187, 3/7/2017 approval). Food was provided to the zebrafish tanks three times daily. Every day, brine shrimp (hatched from INVE artemia cysts) was fed once and flake food twice (Aquatox AX5) supplemented with 7.5% micropellets (Hikari), 7.5% Golden Pearl (300-500 µm, Brine Shrimp Direct) and 5% Cyclo-Peeze (Argent) (Banerji et al., 2016).

Zebrafish strains

C32 and *sof*^{b123} were used (Iovine and Johnson, 2000). We used an equal number of males and females, aged between 6 months and 1 year. For amputation, fish were anesthetized in 0.1% tricaine solution and their caudal fin rays amputated to the 50% level. Regenerating fins at the indicated time points were harvested and fixed in 4% paraformaldehyde (PFA) in phosphate-buffered saline (PBS) overnight at 4°C. After fixation, fins were dehydrated in 100% methanol and stored at −20°C.

Morpholino-mediated gene knockdown

All morpholinos (MOs) used in the experiments were fluorescein-tagged and purchased from Gene Tools. The MOs were reconstituted in sterile water to 1 mM. The *smp-1* MO has been described previously (Kizil et al., 2009). The standard control MO was used as a negative control. Microinjection and electroporation procedures were carried out as described previously (Banerji et al., 2016; Thummel and Iovine, 2017). Briefly, caudal fins were amputated at the 50% level. At 3 days post-amputation (3 dpa), fish were anesthetized and MOs were injected using a Narishige IM 300 Microinjector. Approximately 50 nl of MO was injected per ray into either the dorsal or ventral side of the regenerating fin tissue (the first five or six bony fin rays), keeping the other side uninjected as the internal control. Immediately after injection, both sides of the caudal fin were electroporated using a CUY21 Square Wave electroporator (Protech International) (Banerji et al., 2016). The following parameters were used during electroporation: ten 50 ms pulses of 15 V with a 1 s pause between pulses. After one day post-electroporation (1 dpe), which is equivalent to 4 dpa, the injected side of the fins were evaluated by fluorescence using a Nikon Eclipse 80i Microscope (Diagnostic Instruments) to confirm MO uptake. The MO injected fins were evaluated for regenerate length (4 dpe/7 dpa), segment length (4 dpe/7 dpa), *in situ* hybridization, protein levels by western blot and RNA levels by qRT-PCR.

Regenerate length, segment length and statistics

Fins were calcein stained (Du et al., 2001) before measuring regenerate length and segment length. Briefly, fish were permitted to swim for 15 min in 0.2% calcein (pH 7) at room temperature, and then returned to fresh system water for 10 min. The fish were anesthetized by using tricaine and imaged using Nikon Eclipse 80i Microscope equipped with a SPOT-RTKE digital camera (Diagnostic Instruments) and SPOT software (Diagnostic Instruments). Measurement of regenerate length and segment length were taken on the 3rd fin ray from the ventral- or dorsal-most lobe of the caudal fin, as previously established (Iovine and Johnson, 2000). Measurements were analyzed using Image Pro software. Measurements for regenerate length were considered from the amputation plane to the distal tip of the 3rd fin ray. For segment length, the distance between the first two flanking joints formed following amputation plane was measured on the 3rd fin ray. For each experiment, 7-10 fish were used per trial and at least three independent trials were performed. The SPSS was used to test all data sets for normality. First, skewness and kurtosis values indicated the data did not differ significantly from normality (i.e. z-values were within the range of ±1.96). Second, we completed Shapiro-Wilk's tests (P>0.05) (Razali and Wah, 2011). Student's *t*-test (two-tailed, unpaired) was used to test for statistical differences (P<0.05).

Inhibition of β-catenin activity

IWR-1 was dissolved in DMSO, and this solution was diluted to the appropriate concentration (i.e. 8 or 10 µM) in 500 ml of fish water. XAV939 was dissolved in DMSO and diluted to 5 µM in 500 ml of fish water. Fish with 3 dpa regenerating fins were treated with either IWR-1, XAV939 or DMSO alone at the same concentration as the treatment (with water replacement every 24 h as needed). At the end of the treatment, the skeleton was stained with calcein. Measurements for regenerate length and segment length were collected as described above. Three trials were carried out using five to seven fish per trial.

qRT-PCR analysis

Trizol reagent (Gibco) was used to extract total RNA from a minimum of 10 fins per replicate. Regenerates were harvested with a scalpel under a dissection microscope to ensure only regenerating tissue was collected. For making cDNA, 1 mg of total RNA was reverse transcribed with SuperScript III reverse transcriptase (Invitrogen) using an oligo (dT) primer. The primers (5 mM) for *simplet*, *keratin* (Sims et al., 2009), *evx1* (Dardis et al., 2017) and *axin2* used for qRT-PCR analysis are listed in Table S1. Samples from three independent wild-type, *sof*^{b123}, Smp-KD, standard-control-MO, IWR-1-treated and DMSO-treated RNA samples were prepared. Analyses were performed using the Rotor-Gene 6000 (Corbette Research) and the average cycle number (C_T) was determined for each amplicon. Keratin was used as an internal control (Sims et al., 2009). The delta C_T (ΔC_T) values represent expression levels normalized to keratin values (Banerji et al., 2016). $\Delta\Delta C_T$ values represent the relative level of gene expression. The fold difference was determined using the $\Delta\Delta C_T$ method ($2^{-\Delta\Delta CT}$) as described previously (Ton and Iovine, 2013b). Standard deviation was calculated using the comparative method described in User Bulletin 2 # ABI PRISM 7700 Sequence Detection System (assets.thermofisher.com/TFS-Assets/LSG/manuals/cms_040980.pdf). Student's *t*-tests (two-tailed, unpaired) were performed to test for statistical significance (P<0.05).

In situ hybridization

Antisense digoxigenin-labeled probes were generated as described previously (Kizil et al., 2009 for *smp*; Iovine et al., 2005 for *cx43*; and Ton and Iovine, 2013b for *evx1*). Whole-mount *in situ* hybridization was performed as described previously (Sims et al., 2009). To evaluate the relative level of gene expression, whole-mount *in situ* hybridization was completed on four fins in each of three independent experiments.

Preparation of protein lysates and immunoblotting

Fin lysates were prepared in triplicate as described in the user manual for the Thermo Scientific nuclear and cytoplasmic extraction kit (NE-PER). Fins were amputated at 50% (10 fins for wild type and *sof*) and permitted to regenerate for 3 dpa. For KD analyses, 3 dpa regenerating fins (WT) were injected with either Smp-MO or STD-MO. Fins were harvested at 4 dpa and the fin regenerate tissue was homogenized by a tissue homogenizer (Bio-Gen, PRO 200) at high speed (3) for 5 s with 10 s cooling intervals in the

CER buffer (Thermo Scientific). Homogenized samples were centrifuged at 200 ***g*** for 10 min at 4°C and supernatant protein levels normalized according to Bradford assays. Anti-non-phosphorylated (i.e. active) β-catenin antibody (Cell Signaling, 8814, rabbit mAb used at 1:1000) was used to detect active β-catenin. Lamin a/c (Cell Signaling, 4777S, mouse mAB used at 1:1000) was used as a loading control. Fluorescent secondary antibodies were used for detection (anti-rabbit Alexa-488 at 1:2000 and anti-mouse Alexa 647) in conjunction with Image Lab software (Bio-Rad).

ImageJ software was used to measure the band intensities. Relative pixel densities of gel bands were measured using a gel analysis tool in ImageJ software as described (Banerji et al., 2017). The density of each band was obtained as the area under the curve. For relative density calculation, the density of the active β catenin, lamin a/c bands for the *sof* and Smp-MO lysates was first normalized against the density of the active β catenin, lamin a/c bands from the control samples (i.e. wild type or STD-MO). Relative pixel density was calculated as the ratio of active β catenin and lamin a/c bands. The percentage reduction was calculated by subtracting the relative pixel density from 1 and multiplying by 100. The average percentage reduction with standard deviation is reported in the text. Student's *t*-test (two-tailed, unpaired) was performed on the relative densities to test for statistical significance ($P<0.05$).

Acknowledgements
The authors thank Annie Sanchez for help with *axin2 in situ* hybridization, Rebecca Bowman for care of the zebrafish colony, members of the Iovine lab and the Lehigh University Biological Science Department for supporting this research.

Competing interests
The authors declare no competing or financial interests.

Author contributions
Conceptualization: S.B., M.K.I.; Methodology: S.B., D.G.; Formal analysis: S.B., D.G.; Writing - original draft: S.B.; Writing - review & editing: S.B., D.G., M.K.I.; Supervision: M.K.I.; Project administration: M.K.I.; Funding acquisition: M.K.I.

Funding
This work was supported by the National Institutes of Health grant R15-HD080507 to M.K.I. Deposited in PMC for release after 12 months.

Supplementary information
Supplementary information available online at
http://dev.biologists.org/lookup/doi/10.1242/dev.166975.supplemental

References
Banerji, R., Eble, D. M., Iovine, M. K. and Skibbens, R. V. (2016). Esco2 regulates cx43 expression during skeletal regeneration in the zebrafish fin. *Dev. Dyn.* **245**, 7-21.
Banerji, R., Skibbens, R. V. and Iovine, M. K. (2017). Cohesin mediates Esco2-dependent transcriptional regulation in a zebrafish regenerating fin model of Roberts Syndrome. *Biol. Open* **6**, 1802-1813.
Becerra, J., Montes, G. S., Bexiga, S. R. R. and Junqueira, L. C. U. (1983). Structure of the tail fin in teleosts. *Cell Tissue Res.* **230**, 127.
Chen, B., Dodge, M. E., Tang, E., Lu, J., Ma, Z., Fan, C.-W., Wei, S., Hao, W., Kilgore, J., Williams, N. S. et al. (2009). Small molecule–mediated disruption of Wnt-dependent signaling in tissue regeneration and cance. *Nat. Chem. Biol.* **5**, 100-107.
Dardis, G., Tryon, R., Ton, Q., Johnson, S. L. and Iovine, M. K. (2017). Cx43 suppresses *evx1* expression to regulate joint initiation in the regenerating fin. *Dev. Dyn.* **246**, 691-699.
Du, S. J., Frenkel, V., Kindschi, G. and Zohar, Y. (2001). Visualizing normal and defective bone development in zebrafish embryos using the fluorescent chromophore calcein. *Dev. Biol.* **238**, 239-246.
Funa, N. S., Schachter, K. A., Lerdrup, M., Ekberg, J., Hess, K., Dietrich, N., Honoré, C., Hansen, K. and Semb, H. (2015). β-Catenin regulates primitive streak induction through collaborative interactions with SMAD2/SMAD3 and OCT4. *Cell Stem Cell.* **16**, 639-652.
Govindan, J., Tun, K. M. and Iovine, M. K. (2016). Cx43-dependent skeletal phenotypes are mediated by interactions between the Hapln1a-ECM and sema3d during fin regeneration. *PLoS ONE* **11**, e0148202.
Hoptak-Solga, A. D., Nielsen, S., Jain, I., Thummel, R., Hyde, D. R. and Iovine, M. K. (2008). Connexin43 (GJA1) is required in the population of dividing cells during fin regeneration. *Dev. Biol.* **317**, 541-548.
Huang, S. A., Mishina, Y. M., Shanming, L., Cheung, A., Stegmeier, F., Michaud, G. A., Charlat, O., Wiellette, E., Zhang, Y., Wiessner, S. et al. (2009). Tankyrase inhibition stabilizes axin and antagonizes Wnt signaling. *Nature* **461**, 614-620.
Iovine, M. K. and Johnson, S. L. (2000). Genetic analysis of isometric growth control mechanisms in the zebrafish caudal fin. *Genetics* **155**, 1321-1329.
Iovine, M. K., Higgins, E. P., Hindes, A., Coblitz, B. and Johnson, S. L. (2005). Mutations in connexin43 (GJA1) perturb bone growth in zebrafish fins. *Dev. Biol.* **278**, 208-219.
Jho, E.-H., Zhang, T., Domon, C., Joo, C.-K., Freund, J.-N. and Costantini, F. (2002). Wnt/β-catenin/Tcf signaling induces the transcription of Axin2, a negative regulator of the signaling pathway. *Mol. Cell. Biol.* **22**, 1172-1183.
Kizil, C., Otto, G. W., Geisler, R., Nüsslein-Volhard, C. and Antos, C. L. (2009). Simplet controls cell proliferation and gene transcription during zebrafish caudal fin regeneration. *Dev. Biol.* **325**, 329-340.
Kizil, C., Küchler, B., Yan, J.-J., Özhan, G., Moro, E., Argenton, F., Brand, M., Weidinger, G. and Antos, C. L. (2014). Simplet/Fam53b is required for Wnt signal transduction by regulating β-catenin nuclear localization. *Development* **141**, 3529-3539.
Lin, F.-x, Zheng, G.-z, Chang, C., Chen, R.-c, Zhang, Q.-h, Xie, P., Xie, D., Yu, G.-y, Hu, Q.-x, Liu, D. et al. (2018). Connexin43 modulates osteogenic differentiation of bone marrow stromal cells through GSK3beta/Beta-caatenin signaling pathways. *Cellular Phys and Biochem.* **47**, 161-175.
Liu, G., Luo, G., Bo, Z., Liang, X., Huang, J. and Li, D. (2016). Impared osteogenic differentiation associated with connexin43/microRNA-2016 in steroid induced avascular necrosis of the femoral head. *Exp. Mol. Pathol.* **101**, 89-99.
McMillan, S. C., Zhang, J., Phan, H., Jeradi, S., Probst, L., Hammerschmidt, M. and Akimenko, M. (2018). A regulatory pathway involving retinoic acid and calcineurin demarcates and maintains joint cells and osteoblasts in regenerating fin. *Development* **145**, dev161158.
Moorer, M. C., Hebert, C., Tomlinson, R. E., Iyer, S. R., Chason, M. and Stains, J. P. (2017). Defective signaling, osteoblastogenesis and bone remodeling in a mouse model of connexin 43 C-terminal truncation. *J. Cell Sci.* **130**, 531-540.
Mureli, S., Gans, C. P., Bare, D. J., Geenen, D. L., Kumar, N. M. and Banach, K. (2013). Mesenchymal stem cells improve cardiac conduction by upregulation of connexin43 through paracrine signaling. *Am. J. Physiol. Heart Circ. Physiol.* **304**, H600-H609.
Pacifici, M., Koyama, E., Shibukawa, Y., Wu, C., Tamamura, Y. and Iwamoto, M. (2006). Cellular and molecular mechanisms of synovial joint and articular cartilage formation. *Ann. NY Acad. Sci.* **1068**, 74-86.
Perathoner, S., Daane, J. M., Henrion, U., Seebohm, G., Higdon, C. W., Johnson, S. L., Nusslein-Volhard, C. and Harris, M. P. (2014). Bioelectric signaling regulates size in zebrafish fins. *PLoS Genet.* **10**, e1004080.
Razali, N. M. and Wah, Y. B. (2011). Power comparisons of shapiro-wilk, kolmogorov–smirnov, lilliefors and anderson-darling tests. *J. Statist. Model. Analyt.* **2**, 21-33.
Schulte, C. J., Allen, C., England, S. J., Juarez-Morales, J. L. and Lewis, K. E. (2011). Evx1 is required for joint formation in zebrafish fin dermoskeleton. *Dev. Dyn.* **240**, 1240-1248.
Sims, K., Eble, D. M. and Iovine, M. K. (2009). Connexin43 regulates joint location in zebrafish fins. *Dev. Biol.* **327**, 410-418.
Spagnol, G., Trease, A. J., Zheng, L., Gutierrez, M., Basu, I., Sarmiento, C., Moore, G., Cervantes, M. and Sorgen, P. L. (2018). Connexin43 carboxyl-terminal domain directly interacts with β-catenin. *Int. J. Mol. Sci.* **19**, 1562.
Stewart, S., Gomez, A. W., Armstrong, B. E., Henner, A. and Stankunas, K. (2014). Sequential and opposing activities of Wnt and BMP coordinate zebrafish bone regeneration. *Cell Rep.* **6**, 482-498.
Stoick-Cooper, C. L., Weidinger, G., Riehle, K. J., Hubbert, C., Major, M. B., Fausto, N. and Moon, R. T. (2007). Distinct Wnt signaling pathways have opposing roles in appendage regeneration. *Development* **134**, 479-489.
Thermes, V., Candal, E., Alunni, A., Serin, G., Bourrat, F. and Joly, J. S. (2006). Medaka simplet (FAM53B) belongs to a family of novel vertebrate genes controlling cell proliferation. *Development* **133**, 1881-1890.
Thummel, R. and Iovine, M. K. (2017). Using morpholinos to examine gene function during fin regeneration. *Methods Mol. Biol.* **1565**, 79-85.
Tu, S. and Johnson, S. L. (2011). Fate restriction in the growing and regenerating zebrafish fin. *Dev. Cell* **20**, 725-732.
Ton, Q. T. and Iovine, M. K. (2012). Semaphorin3d mediates Cx43-dependent phenotypes during fin regeneration. *Dev. Biol.* **366**, 195-203.
Ton, Q. V. and Iovine, M. K. (2013a). Determining how defects in connexin43 cause skeletal disease. *Genesis* **51**, 75-82.
Ton, Q. V. and Iovine, M. K. (2013b). Identification of an evx1-dependent joint-formation pathway during FIN regeneration. *PLoS ONE* **8**, e81240.
Wehner, D., Cizelsky, W., Vasudevaro, M. D., Özhan, G., Haase, C., Kagermeier-Schenk, B., Röder, A., Dorsky, R. I., Moro, E., Argenton, F. et al. (2014). Wnt/β-catenin signaling defines organizing centers that orchestrate growth and differentiation of the regenerating zebrafish caudal fin. *Cell Rep.* **6**, 467-481.
Westerfield, M. (1993). *The Zebrafish book*. Eugene: University of Oregon Press.
Xia, X., Batra, N., Shi, Q., Bonewald, L. F., Sprague, E. and Jiang, J. X. (2010). Prostaglandin promotion of osteocyte gap junction function through transcriptional regulation of connexin43 by glycogen synthase kinase 3/β-catenin signaling. *Mol. and Cell. Biol.* **30**, 206-209.
Yamagami, T., Molotkov, A. and Zhou, C. J. (2009). Canonical Wnt signaling activity during synovial joint development. *J. Mol. Hist.* **40**, 311-316.

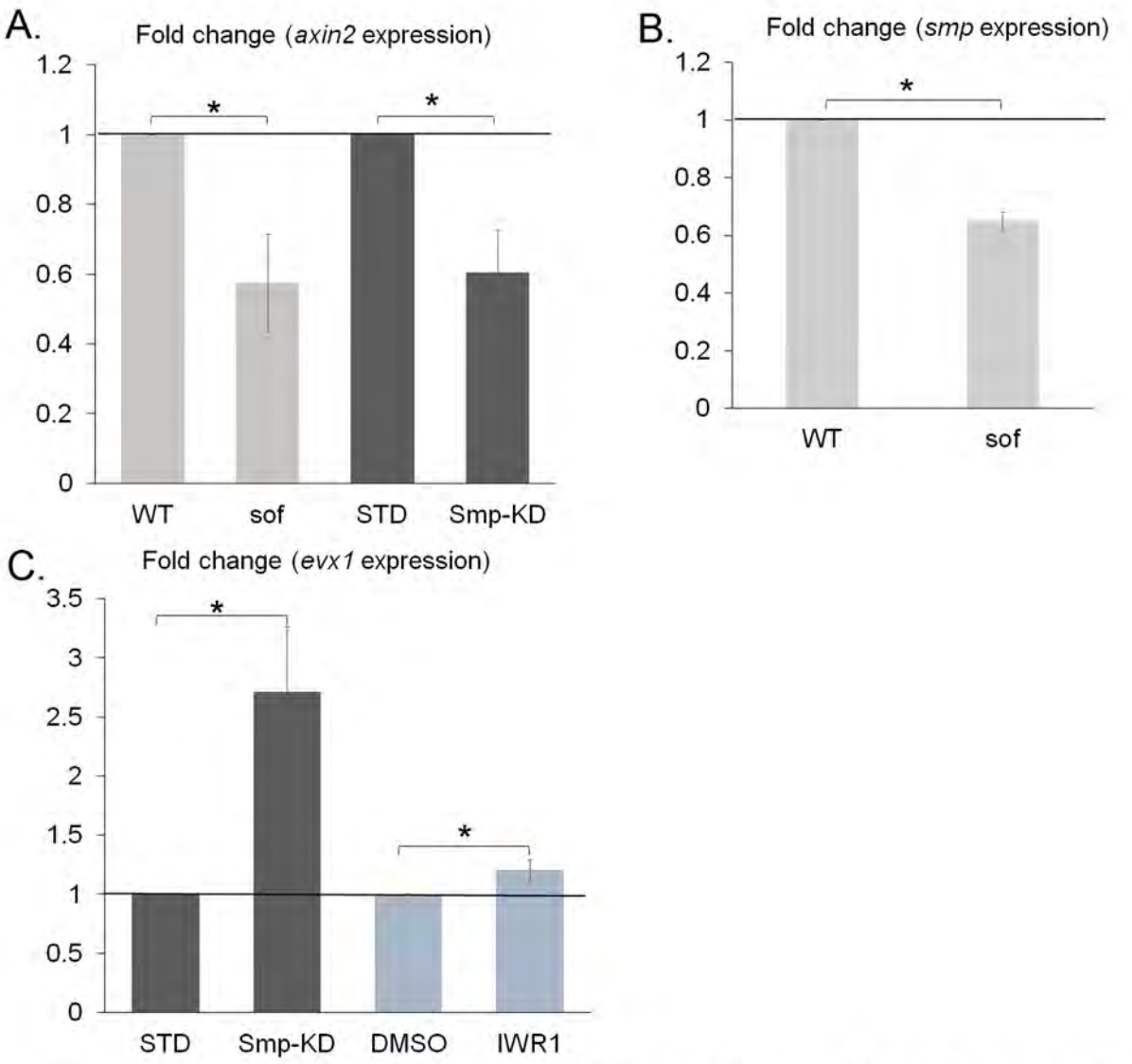

Figure S1: Graphical representation of qRT-PCR data shown in Table 1. Experimental samples are compared to control samples that represent a value of one (horizontal line in each graph). (A) *axin2* expression is significantly reduced in sof^{b123} compared to WT, and in Smp-KD compared to and STD. (B) *smp* expression is significantly reduced in sof^{b123} compared to WT. (C) *evx1* expression is significantly increased in Smp-KD fins compared to STD, and in IWR1-treated fins compared to DMSO-treated fins. For all samples, the data did not differ significantly from normality (Shapiro-Wilk's test $p>0.05$). Error bars represent the standard error. Brackets identify groups that were compared for statistical analysis and * represents statistical significance of $p < 0.05$ (Student's t-test).

Table S1: Primers used in this study

Gene	qRT-PCR	In- situ Primers	Morpholino	Morpholino effiency primer
smp	Forward primer: 5' ATCAGAAGATCGGC GTCAAG3' Reverse primer: 5'GGACAGCTGAGAC TGTGAAA3'	Forward primer:5'CAGAGAGGAGTCTTCAAT CCATCAG-3' Reverse primer: 5'TAATACGACTCACTATAGGGAGA AATGCTTCTCAGTTCCTCTCAA3' (Kizil *et al.,* 2009)	5′GAATATCTG CACTTACCCA TGATTC3′ (Kizil *et al.,* 2009)	C1 Forward primer: 5'CAGATGTTGGGAG TGTGTGT3' C2 Reverse primer:5'ATGGGAAA CCGTGAGTGAAG3' P1 Forward Primer: 5'GAAGGCGGTTGAC GATGTAA3' P2 Reverse primer:5'CAGGAAAG CCTGATGGATTGA3'
axin2	Forward primer:5'CAATGGACG AAAGGAAAGATC3' Reverse primer: 5'AGAAGTACGTGAC TACCGTC3'	Forward primer: 5' AGATGACCCACGTCCACCGG Reverse primer T7: 5'TAATACGACTCACTATAGGGAGA GACACTTGGCCGTTCATCC3'		
evx1	Forward primer: 5'TTGGCGGCTGCCT TAAATT3' Reverse primer: 5'TGTCCTTCATGCGA CGGTT3' (Dardis et al., 2017)	Forward primer- 5'TAATACGACTCACTATAG3' Reverse primer-T3- 5'GGATCCATTAACCCTCACTAAAG GGAAGAGCTATGACGTCGCAT3' (Dardis et al., 2017)		
ker4	Forward primer: 5'TCATCGACAAAGT GCGCTTC3' Reverse primer: 5'TCGATGTTGGAAC GTGTGGT3'			